Heating Pulse Tests under Constant Volume on Natural Boom Clay. Experimental Results and Numerical Simulations

Analice Lima[1], Enrique Romero[1], Jean Vaunat[1], Antonio Gens[1] & Xiangling Li[2]

[1] Universitat Politècnica de Catalunya, Barcelona, Spain
[2] EIG EURIDICE/SCK•CEN, Mol, Belgium

Summary

Boom clay is a potential geological host formation for High Level Nuclear Waste in Belgium. Impact of thermal loads may play an important role on this clay formation. To this aim, heating pulse tests on intact borehole samples were carried out using an axi-symmetric heating cell. Heating tests under nearly constant volume conditions and different target temperatures (maximum 85°C) were performed under controlled hydraulic boundary conditions. Selected test result are presented and afterwards calibrated and simulated using CODE_BRIGHT.

1. Introduction

Natural Boom clay is the subject of extensive research in Belgium dealing with all phenomena that may possibly affect the performance of this clay as potential geological host formation for High Level Nuclear Waste. Specifically, thermal loads may play an important role on this low-permeability clay. There are a number of laboratory results concerning the saturated hydro-mechanical behaviour of natural Boom clay under constant temperature field and studies on this area are described in De Bruyn (1996)[1], Sultan (1997)[2] and Le (2008)[3]. Nevertheless, information on clay hydro-mechanical response on heating and cooling paths under small-scale laboratory conditions is less known. To this end, the paper explores the consequences of thermal loads by presenting selected results of a comprehensive test programme performed on an axi-symmetric heating cell described in Muñoz *et al.* (2009)[4]. This cell was improved to achieve higher temperatures.

Heating and cooling tests –maximum temperature was limited to 85°C– on borehole samples were performed under nearly constant volume and controlled hydraulic boundary conditions: constant water pressure at the bottom drainage and top end with no flow condition. Selected test result are presented and discussed in terms of the joint measurements of temperature and pore water pressure along different heating and cooling paths. In order to simulate test results, the program CODE_BRIGHT (Olivella *et al.* 1996 [5]) was used. The paper shows the calibration of thermal properties and the simulation of selected thermal results.

2. Experimental programme

2.1 Tested material

Laboratory tests were performed on natural Boom clay (Mol, Belgium). Table 1 summarises some properties of this slightly overconsolidated Tertiary clay (20%-30% kaolinite, 20%-30% illite and 10%-20% smectite). A soil specimen was trimmed from a borehole sample retrieved in horizontal

direction with dimensions 75 mm in diameter and 100 mm high (bedding planes are parallel to the cell axis).

Table 1. Some properties of Boom clay. Lima et al. (2008)[6].

Property	Value
Gravimetric water content, w	21 to 25%
Void ratio, e	0.560 to 0.618
Degree of saturation, S_r	91 to 100% (*)
Vertical water permeability (20ºC), k_{wv}	$(2.4$ to $3.1) \times 10^{-12}$ m/s
Vertical water permeability (80ºC), k_{wv}	6.5×10^{-12} m/s
Horizontal water permeability (20ºC), k_{wh}	$(5.7$ to $7.4) \times 10^{-12}$ m/s
Horizontal water permeability (80ºC), k_{wh}	1.26×10^{-11} m/s

(*) laboratory samples are not fully saturated due to some water content loss on storage

2.2 Laboratory equipment and tests protocols

Figure 1 shows a modified scheme of the axi-symmetric heating cell described in Muñoz *et al*. (2009)[4]. A controlled-power heater (*H* in Fig. 1) is installed along the axis of the sample in the lower part of the cell. Different transducers are monitoring the sample response: two miniature pore water pressure transducers (*Pw₁* and *Pw₂* in Fig. 1), three thermocouples (*T₁*, *T₂* and *T₃*), and top and lateral strain gauges attached to reduced thickness sections (*SG*). Moreover, the cell has top and bottom valves (u_u and u_b) to apply the hydraulic conditions. The cell was updated to perform heating paths at temperatures higher than 50ºC.
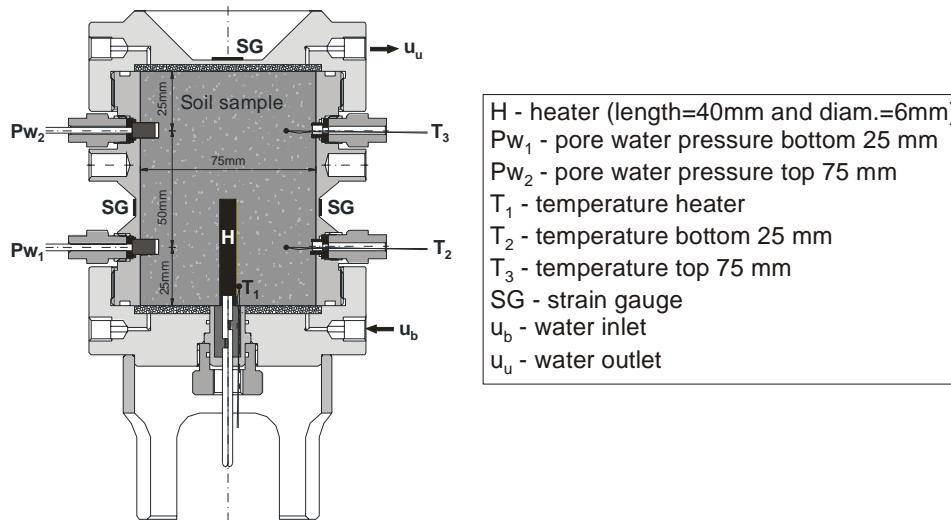

Figure 1: Modified scheme of the heating cell (adapted from Muñoz et al. 2009[4]).

The protocol of the tests presented three important phases: hydration, heating and cooling. Throughout the heating and cooling phases, the bottom drainage was maintained open at a constant water pressure of 1 MPa using an automatic pressure / volume controller, while the upper valve was kept closed. This backpressure is important since it allows measuring the pore pressure drop during the cooling phase while avoiding negative pressures (below atmospheric conditions). The initial and external temperatures were always regulated by submerging the cell inside a temperature controlled water bath at 19ºC. The heater with controlled power supply remained switched on for 24 hours during the heating phase and later switched off to perform the cooling phase. Tests ended when soil temperature reached the initial condition (around 19ºC).

3. Experimental results

This work presents the results obtained along the thermal stage 4, in which the heater reached a maximum temperature of 85ºC as a consequence of being supplied by a constant power of 19 W (Fig. 2). Figure 2a presents the time evolution of temperature recorded by a thermocouple placed very near the heater (T_1 in Fig. 1), whereas Fig. 2b shows the time evolution of the corresponding water pressure changes (Pw_1 and Pw_2). Maximum pressure build-up during the initial quasi-undrained heating stage was 1.83 MPa at Pw_2 and slightly lower at Pw_1 (1.69 MPa), which is placed near the bottom draining boundary. During quasi-undrained cooling, while returning to the initial temperature, the pore water pressure dropped to 0.13 MPa at Pw_2 and to 0.17 MPa at Pw_1. As observed, quite symmetric pressure peaks were obtained in both heating and cooling stages. It appears that key hydro-mechanical properties linked to this phenomenon are preserved after the initial heating stage, at least within this initial thermal cycle. Maximum values of the quasi-undrained pressurisation coefficients –defined as the pore pressure increase/decrease due to a unit temperature increase/decrease– were 0.189 MPa/ºC on heating and slightly lower 0.108 MPa/ºC on cooling.

During heating, pore water pressure increased due to its larger thermal expansion coefficient. The magnitude of the water pressure change depends on the rate and range of temperature increase / decrease (quasi-undrained heating and temperature dependence of the water thermal expansion coefficient), on the soil compressibility (dependent on the stress state) and thermal-expansion coefficient, the water permeability and porosity (also dependent on the stress sate), the induced damage due to pore pressure increase, as well as on the hydraulic boundary condition applied. The change of pore water pressure on thermal loading under saturated conditions has been analysed assuming volumetric compatibility between soil matrix and their constituents (liquid and solid) using compressibility and thermal expansion coefficients (refer for example to Agar *et al*. 1986 [7]). As previously indicated, a larger pressure build-up is detected at Pw_2, due to the fact that the measuring point is located at a larger distance from the draining boundary. After the heating path, pore water pressures dissipate at constant temperature towards the value applied by the hydraulic boundary conditions. Pore water pressure Pw_2 dissipates more slowly due to its larger distance to the draining boundary.
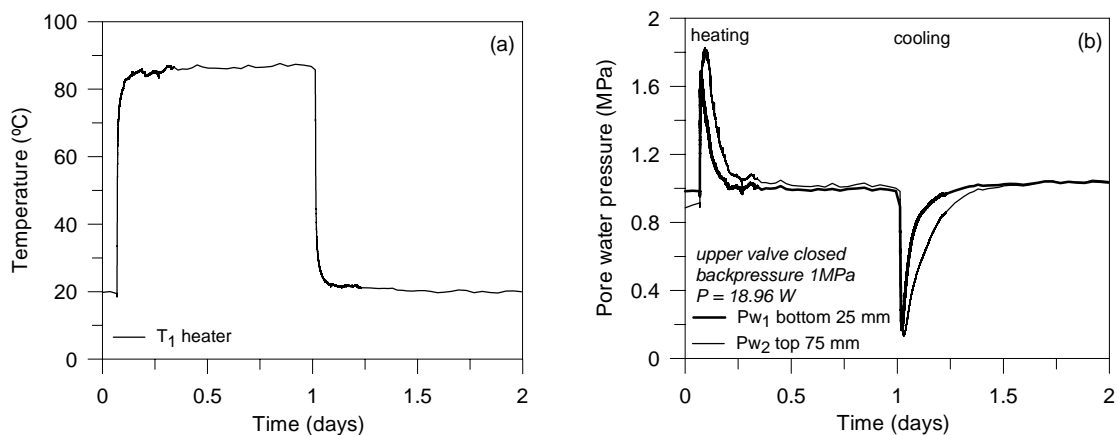

Figure 2: Stage 4. (a) Time evolution of temperature. (b) Time evolution of pore water pressures.

4. Numerical simulations

4.1 Material parameters and boundary conditions

The finite element program CODE_BRIGHT (Olivella *et al.* 1996[5]) was used to perform the calibration and simulation of thermal results. The program solves in a monolithic and coupled way the mass balance equations of solid, water and air, the balance of energy and the equilibrium conditions. For this particular case, in which only temperature is analysed –stress equilibrium and mass balances have no important influence–, the internal energy balance was solved considering full saturation, neglecting the convective liquid flux due to the low permeability of the soil and disregarding the convective flux of solids because of the no volume change condition.

Five materials were considered in the simulation: soil, stainless steel, heater, porous disks and epoxy resin. Figure 3 shows the axisymmetric geometry along the vertical axis and the materials, together with the finite element mesh used. Soil and stainless steel thermal properties are also included (solid phase specific heat, C_s, and thermal conductivity, λ). The boundary conditions include a convection coefficient, h, controlling thermal flux at the interface from the cell to the boundary (at prescribed temperature), and the power source term 13.94×10^6 $Js^{-1}m^{-3}$.
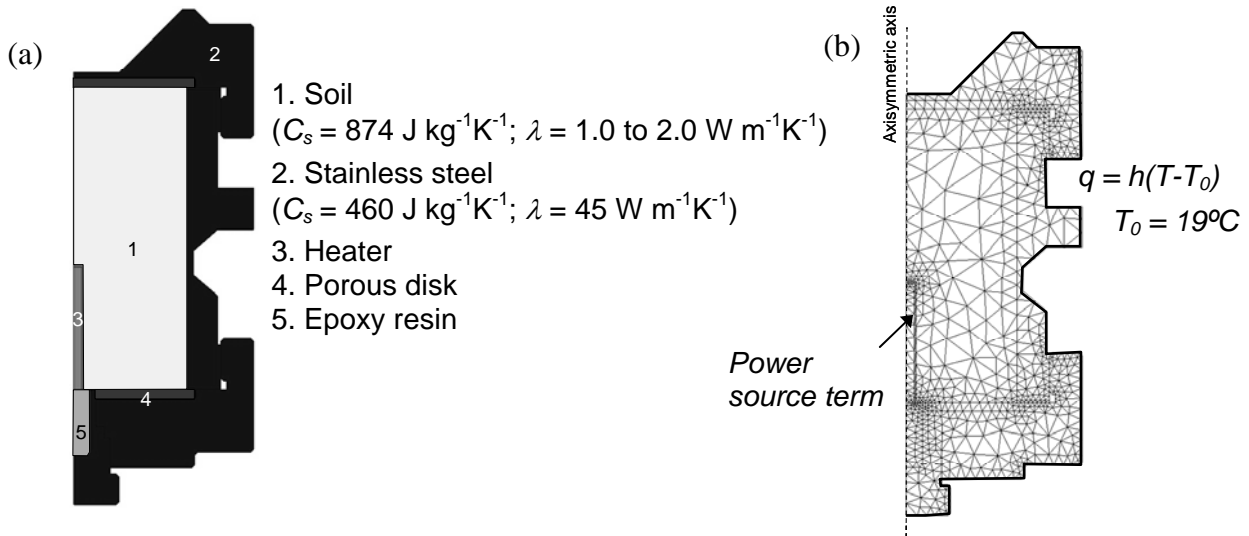

Figure 3: (a) Geometry and materials. (b) Finite element mesh and boundary conditions.

4.2 Calibration and simulation results

A minimisation algorithm to determine soil thermal conductivity, λ, and the convection coefficient, h, was followed to find the best fit between measured and simulated temperatures. To this aim, 104 calculations were performed and the back-analysed values were $\lambda=1.6$ $Wm^{-1}K^{-1}$ and $h=24$ $Wm^{-2}K^{-1}$. Figure 4 on the left shows the time evolution of temperatures (experimental and simulated results) near the heater (T_1 in Fig. 1), at the bottom (T_2 in Fig. 1) and at the top (T_3 in Fig. 1). Figure 4 on the right shows the temperature field inside the cell at the maximum temperature of the heater and under steady state conditions.
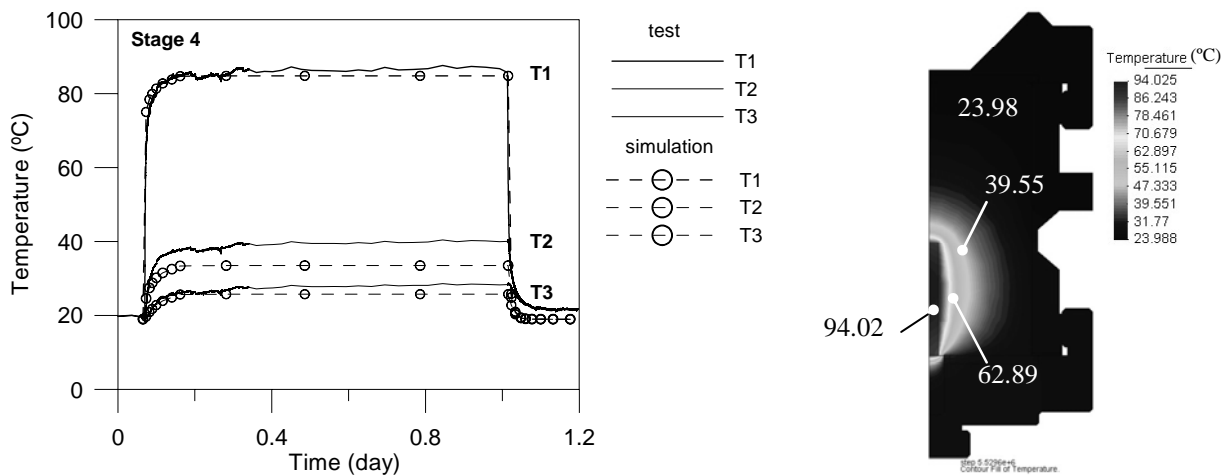
Figure 4: Temperature evolution at different locations and along stage 4 (experimental and simulated results). Temperature field inside the cell at maximum heater temperature.

5. Conclusions

A series of heating and cooling paths were performed on natural Boom clay to study the consequences of thermal loads on this clay formation. Tests were performed in a fully-instrumented heating cell –with several thermocouples and pressure transducers– under nearly constant volume and controlled hydraulic boundary conditions: constant water pressure at the bottom drainage and top end with no flow condition. Selected results of a comprehensive experimental programme on intact borehole samples retrieved in the horizontal direction were presented and discussed in terms of the joint measurements of temperature and pressure changes during the application of a heating-cooling cycle.

In a first stage, thermal test results were interpreted and simulated using CODE_BRIGHT. After a first calibration by back-analysis of some thermal properties (thermal conductivity of the soil and convection coefficient, which controlled thermal flux at the interface from the heated cell to the boundary), selected time evolutions of temperatures at different locations were successfully simulated along a heating and cooling cycle. In a future stage, the extensive data collected will be used to calibrate the hydraulic properties by gathering joint thermal, hydraulic and mechanical results with the same numerical code.

6. Acknowledgements

References

[1] De Bruyn, D. and Thimus, J.-F. (1996). The influence of temperature on mechanical characteristics of Boom clay: The results of an initial laboratory programme. *Engineering Geology*, 41: 117-126.

[2] Sultan, N. (1997). Etude du comportement thermo-mécanique de l'argile de Boom: expériences et modélisation. PhD Thesis, CERMES, Ecole Nationale des Ponts et Chaussées, Paris.

[3] Le, T.T. (2008). Comportement thermo-hydro-mécanique de l'argile de Boom. PhD Thesis, CERMES, Ecole Nationale des Ponts et Chaussées, Paris.

[4] Muñoz, J.J., Alonso, E.E. and Lloret, A. (2009). Thermo-hydraulic characterization of soft rock by means of heating pulse tests. *Géotechnique*, 59(4): 293–306.

[5] Olivella S., Gens A., Carrera J. and Alonso E.E. (1996). Numerical formulation for a simulator (CODE_BRIGHT) for the coupled analysis of saline media. *Int. Journal Engineering Computations*, 13 (7): 87 - 112.

[6] Lima, A., Romero, E. and Pineda, J.A. (2008). Low-strain shear modulus dependence on water content of a natural stiff clay. XIV Congresso Brasileiro de Mecânica dos Solos e Engenharia Geotécnica, Búzios, Rio de Janeiro, Brazil. Associação Brasileira de Mecânica dos Solos e Engenharia Geotécnica: 1763-1768.

[7] Agar, J.G., Morgenstern, N.R. and Scott, J.D. (1986). Thermal expansion and pore pressure generation in oil sands. *Can. Geotech. J.*, 23: 327-333.